sustainability

MDPI

Article

Alkali Activation of Clay and Water Potabilization Sludge Binary Blends: Influence of Composition and Curing Conditions

Marina Clausi, Gianluca Girardi and Daniela Pinto *

Earth and Geoenvironmental Sciences Department, University of Bari Aldo Moro, 70121 Bari, Italy; marina.clausi@uniba.it (M.C.); g.girardi8@studenti.uniba.it (G.G.)
* Correspondence: daniela.pinto@uniba.it; Tel.: +39-080-5442604

Abstract: This work aims to evaluate the compatibility and features of alkali-activated blends obtained by replacing carbonate-rich illitic clay with either untreated or heat-treated water potabilization sludge (WPS). The experimental setting was created looking towards producing environmentally friendly solutions such as precursors that are sourced from the same territory, room-temperature curing in realistic environmental conditions, and activation exclusively with sodium hydroxide (NaOH) solutions. A multi-analytical characterization of the blends using X-ray powder diffraction (XRPD), an optical microscope (OM), a scanning electron microscope (SEM) equipped with an energy dispersive spectrometer (EDX), and a mechanical test demonstrated that up 75% of calcinated sludge and 25% of uncalcinated sludge could be successfully incorporated into the clay-based blends, offering a valuable alternative to landfill disposal of WPS. The matrices' features were affected both by the amount of sludge in the blends and by the environmental conditions curing. since mineralogical investigations, OM and SEM observations showed the formation of secondary crystalline phases, mainly zeolitesin addition to amorphous gel. The mechanical strength results reached values between ~3 and 9 MPa, suggesting the possible use of the investigated alkali-activated blends for the formulation of precast building materials. Furthermore, to assure the replication of these alkali-activated blends, uncontrolled (T °C and RH%) curing does not appear to be the most appropriate solution. The study demonstrated that WPS, traditionally destined for landfill, could be a resource for the production of alkaline-activated materials by partially replacing unrenewable raw materials. thus resulting in the creation of eco-sustainable and economic processes as WPSare a widely and locally available industrial byproduct. However, a better control of mix designs and curing conditions is necessary for the upscaling of the here investigated blends.

Keywords: alkali activation; amorphous gel; carbonate-rich clay; environmental curing; water potabilization sludge; zeolites

Citation: Clausi, M.; Girardi, G.; Pinto, D. Alkali Activation of Clay and Water Potabilization Sludge Binary Blends: Influence of Composition and Curing Conditions. *Sustainability* **2023**, *15*, 16623. https://doi.org/10.3390/su152416623

Academic Editor: Syed Minhaj Saleem Kazmi

Received: 27 October 2023
Revised: 24 November 2023
Accepted: 1 December 2023
Published: 7 December 2023

1. Introduction

Alkali-activated materials (AAMs) and their sub-category known as geopolymers have emerged as low-carbon materials with great potential in terms of their mechanical, technological, and sustainable properties, showing technical characteristics that are similar to, and sometimes higher than, Portland cement and other carbonate-based binders [1,2].

AAMs are defined as inorganic polymers originating from the interaction of aluminosilicate powders with alkaline activators (in solid or liquid phase), at near-ambient conditions, and the consequent condensation of the resulting blend in a solid 3D network [3,4]. Different authors proposed detailed descriptions of alkali activation reactions [4–6] as well as the progress in this field of investigation [1,7,8].

Alkali activation technology is particularly versatile and allows for varied raw materials, mix designs, and synthesis parameters to obtain materials with a wide range of

properties [8–10]. In particular, the type of precursor strongly influences the properties and the possible applications of AAMs. Among the natural resources, clays are well-known precursors to, especially, kaolinitic clays [11,12], although the use of non-kaolinitic clays has been rapidly growing in recent years [13–18]. Different authors have proposed the valorisation of local resources as a strategy for the transition towards a sustainable raw materials supply chain [19]. D'Elia et al. [20,21] demonstrated the suitability of carbonate-rich illitic clay sediments from the Apulian territory, Italy as raw materials for the preparation of AAMs after both thermal and mechanical pre-treatment. More recently, promising results were obtained by blending this carbonate-rich illitic clay with fly ash and blast furnace slag [22], two byproducts obtained from coal combustion power plants and iron-making process, respectively.

The reuse of waste and industrial byproducts in the substitution of natural precursors in AAM production is nowadays becoming a widely explored research field [23–25], since any natural or man-made material which contains sufficient reactive silica and alumina could be a suitable precursor in the alkali activation process. This makes this technology of great ecological relevance, according to EU recommendations on sustainability and circular economy (https://environment.ec.europa.eu, accessed on 26 October 2023). In fact, more sustainable practices nowadays imply a shift from a linear model to a circular model [26], modifying the idea of end-of-life, in which waste is normally disposed in landfills or dispersed in the environment, to that of end-of-waste by reusing and recycling products.

The reuse of water potabilization sludge (WPS) that has already been tested for the synthesis of zeolites [27,28] or for the use as supplementary construction materials [29,30] in recent years has been successfully proven to produce AAMs [31–38]. This waste is produced from the water potabilization process, consisting of a set of treatments in which the water from reservoirs is processed to become drinkable. In particular, they are generated during the clarification–flocculation phase, when alumina-based coagulants, such as aluminium chloride ($AlCl_3$) or aluminium polychloride ($Al_n(OH)_mCl_{3n-m}$), are added, so generating an aluminium-rich suspension which represents a solid fraction separated from the water. As a whole, WPS is mainly composed of clayey sediments, sand, and an organic fraction [39] with Si and Al being the main chemical components, followed by Ca, Fe, Mg, Na, K, Ti, and P [40]. However, the composition of WPS is generally influenced by several factors, such as the geological context of reservoirs, the quality of raw water, and the volume of treated water, along with the treatment processes [34,39], making a compositional standardisation of this type of waste difficult to obtain [41]. WPS is produced continuously because the water potabilization process is currently fundamental and unstoppable for humans, so a significant volume of this waste is potentially available to be reused every year instead of being conventionally disposed in landfills [29,42].

In this study, alkali-activated materials were synthesised for the first time using blends of local carbonate-rich illitic clays and WPS- from the Apulian plant of Locone, Minervino Murge, Italy, in order to investigate the features and properties of alkali-activated binders (AABs) obtained by the progressive replacing of this natural and unrenewable resource with a waste material coming from the same territory (the Apulia region, Italy). Thus, this study has great relevance in the perspective of the reduction of the supplying and hauling distances of raw materials, as well as the exploitation of alternative supply resources that may preserve natural resource consumption by promoting pragmatical proposals of circularity that are also consistent with the concept of the three 'Rs', recovery, recycle, and reuse [40].

Considering the literature, it is possible to find some studies that already address the topic of AABs production by replacing clay with WPS. For example, Messina and co-authors [34] obtained precast geopolymer blocks from the alkali activation of calcined WPS and clay sediments (1:1 ratio) with sodium silicate solution and standard sand. In their preliminary tests, slight differences in terms of mechanical strength were observed to vary the curing temperature (20–60 °C). Geraldo et al. [33] investigated geopolymer mortars from uncalcined WPS (up to 60%), metakaolin and a sodium silicate solution from

rice husk ash, noting a decreasing of workability and mechanical properties as WPS content increase. However, the use of sodium silicate as an activating solution should be avoided whenever it is possible as it significantly decreases the significance of geopolymers as green and sustainable materials. The synthetization process of sodium silicate has, in fact, a large carbon footprint, as it is based on the fusion of siliceous sand with anhydrou sodium carbonate (Na_2CO_3) at temperatures of >1.000 °C [43].

Manosa et al. [31] studied uncalcined WPS clay systems activated using NaOH and cured at 80 °C, reaching a promising formulation with a WPS content of 20%, but they showed that the availability of SiO_2 and Al_2O_3 from the two untreated precursors was too low, hence most of the precursors remained unreacted and the amount of newly formed binder phases was low.

Starting from the results of the available literature, a number of different experimental set-ups have been selected and tested in this study with the aim of reducing the carbon footprint of the synthetization process and, thus, supporting the transition toward more sustainable processes. Hence, alkali activation was promoted for both heat-treated and untreated WPS exclusively using sodium hydroxide solutions instead of less sustainable alkaline silicate. Furthermore, room-temperature curing was used with the dual purpose of avoiding energy-expensive procedures and evaluating the binders' behaviour in realistic environmental conditions. In this connection, one of the most interesting novelties of this work is represented by the curing of alkaline-activated pastes under two completely different room temperature conditions (i.e., during summers with external temperatures greater than 35 °C and high humidity and during winter seasons with temperatures ranging from 10 °C to 20 °C and low degrees of humidity) to evaluate the effect of the actual climatic conditions during environmental temperature curing.

All of the samples were characterized by a multi-analytical approach including compressive strength measurements, X-ray powder diffraction (XRPD), Optical Microscope (OM), and Scanning Electron Microscope (SEM) equipped with an Energy-Dispersive spectrometer (EDX) to evaluate the compatibility of the studied clay -WPS system and the optimal percentage of WPS for clay substitution to obtain samples with the best characteristic in terms of physical and chemical properties. The obtained results were compared with the existing literature for a critical review.

2. Materials and Methods

2.1. Selection of Raw Materials

The water potabilization sludge used in this work comes from the water treatment plant of Locone (Minervino Murge, Apulia region, Italy), which processes water coming from the Locone torrent, collected from the homonymous artificial reservoir. The mineralogical and chemical compositions of the sludge can be found in Clausi & Pinto, 2023 [41]. The WPS- was dried for 24 h in a laboratory stove at 105 °C, as it was quite moist when collected, and used untreated (labelled LOCtq) or after a thermal treatment at 700 °C for 1 h (LOC700), according to results reported in [41]. Both the sludge samples were pre-milled at 300 rpm, t = 2 min to reduce particle size (<1 mm) and ground at 300 rpm, t = 30 min, using the Pulverisette 5 planetary mill with agate jars from Fritsch (Idar-Oberstein, Germany).

The carbonate-rich illitic clay (labelled MA57) used in this study was collected from a clay deposit located in Lucera (Apulia region, Italy) and belongs to the sub-Apennine clay formation [44]. In-depth mineralogical and chemical characterizations of this clay have been reported in previous studies [20–22]. The most effective activation method of increasing the reactivity of this clay was shown to be a combination of grinding and heating [20]. Thus, a combined mechanical (conventional ball mill) and thermal (700 °C for 1 h) treatment was used prior to its use, according to the procedure used in [22].

2.2. Sample Preparation

For the synthesis of the alkali-activated samples, the following procedure was used and repeated for each sample:

(1) Powders of LOCtq, LOC700, and MA57 were mixed in different weight proportions (0/100; 25/75; 50/50; 75/25) in a mechanical mixer for 5 min to create homogeneous powder blends.
(2) A sodium hydroxide (NaOH) solution 6 M (mad from pellets of sodium hydroxide (Sigma-Aldrich, St. Louis, MO, USA, purity $\geq$ 98%)) was added slowly to the powder in order to permit facilitate the reaction. The concentration of the activating solution was chosen based on the findings of [21,22,41].
(3) The mixing operations were performed by using a mechanical stirrer for 5 min at 1200 rpm.
(4) The blends were poured into cubic steel moulds (40 $\times$ 40 $\times$ 40 mm^3) and compacted by mechanical vibrations for 60 s by using a vibratory plate to remove entrained air.
(5) The samples were cured at room temperature in sealed vessels for 24 h to ensure 100% relative humidity (R.H.) before being demoulded and left in environmental conditions for 28 days [23,24,43]

In order to evaluate the effect of the actual climatic conditions during the environmental temperature curing, a first set of samples was prepared during the summer season (ss), under very hot external temperatures (more than 35 °C) in an environment with no air conditioning, whereas a second set of samples was prepared during the winter season (ws) under temperate climatic conditions (external temperature from 10 °C to 20 °C).

2.3. Characterization Methods

The chemical composition of WPS was determined by X-ray fluorescence (XRF) using a Panalytical AXIOS Advanced (PAN Alytical, Almelo, The Netherlands) automatic spectrometer, equipped with an X-ray tube X SST-mAX (Rh anode). The detection limit for major element oxides was 0.01 wt%. Oxide concentrations was determined on powder pellets obtained by pulverizing 5 g of the sample with an Elvacite polymer resin dissolved in acetone and pressing under a hydraulic press for 15 s at 15 ton/m^2. Loss on ignition (L.o.I.), determined by mass losses at 950 °C, was used to measure the volatile components.

The particle size distributions of MA57, LOCtq, and LOC700 were determined in water using a Mastersizer 3000 (Malvern Instruments, Malvern, UK) laser diffractometer (measuring range of 0.01 µm–3.5 mm) equipped with a HydroEV dispersion unit according to the indications of reference standard ISO 13320 [45].

Mineralogical characterizations of precursors and alkali-activated samples (at 28 days of curing) were performed using X-ray powder diffraction (XRPD) which was conducted with a PANalytical Empyrean diffractometer (Malvern, PANalytical, Almelo, The Netherlands) equipped with a real time multiple strip (RTMS) PIXcel^{3D} detector and Cu-Kα radiation. The operating conditions were 40 kV and 40 mA, range was 3–70° 2θ, virtual scan was 0.026° 2θ, and counting time was 120 s per step. The incident beam pathway included a 0.125° divergence slit, a 0.25° antiscattering slit, and a soller slit (0.02 rad), whereas a Ni filter, a soller slit (0.02 rad), and an antiscatter blade (7.5 mm) were mounted in the diffracted pathway. X-ray patterns were analysed using the software X'Pert High Score version 3.0 e (Malvern PANalytical, Almelo, The Netherland) which includes the ICSD database. Quantitative phase analyses (QPA) [46] was carried out using the Rietveld method by means of the Rietveld refinement software BGMN version 5.1.8 (J. Bergmann, Dresden, Germany) [47], implemented in the graphical user interface Profex version 4.3.2 [48].

A Stereomicroscope Leica EZ4 W (Leica Microsystems, Wetzlar, Germany), with a built-in 5-megapixel camera with a 2592 $\times$ 1944-pixel resolution and a magnification range of 8×–35× was used on the cut sections of the alkali-activated samples at 28 days of curing to evaluate their micro-textural features.

A scanning electron microscope (SEM) LEO model EVO-50XVP (Zeiss, Cambridge, UK), coupled with an X-max (80 mm^2) Silicon drift Oxford instruments detector EDX system (SEM-EDX) (Oxford Instruments, High Wycombe, UK), was used for investigating the alkali-activated samples. The measurements were performed on carbon-coated fragments fixed on a metal support by using carbon tape. Analyses were performed, in vacuum mode,

and images were collected using a secondary electron (SE) at working distances between 7.5–8.5 mm with an acceleration voltage of 10–15 kV and a beam current of 10 µA. EDX analyses were done with an accelerating voltage of 10–15 kV on spots and on variable areas, acquiring a minimum of 60 s per spot analysis. Chemical compositions were determined considering 100 wt% oxide content on an H_2O- and CO_2-free basis.

Compressive strength was measured at "Tecno-Lab s.r.l." laboratory in Altamura (Bari, Italy) using a Matest E161-PN291 (Matest, Bergamo, Italy) testing machine, with a load cell of 250 kN and a displacement speed of 2.4 kN/s The compression process was performed according to UNI EN 196-1:2016 on 3 replicas for each type of sample.

To obtain immediate feedback on the products stability, a chemical stability test, also known as an integrity test, was performed on the newly cured samples by immersing them in distilled water (weigh ratio sample/water 1:10) at room temperature for 24 h [49]. A structural stability test was also conducted by keeping samples soaked in water for a further 10 days.

3. Results and Discussion

3.1. Precursors Characterization

The chemical composition of the clay precursor (MA57) and the sludge (LOCtq), determined by XRF, is reported in Table 1. MA57 shows SiO_2 (42 wt%) and CaO (27 wt%) as the main oxides due to the enrichment in carbonates ofthe clay. The low value of loss on ignition is due to its heat treatment at 700 °C.

Table 1. Bulk chemical (XRF) composition and mineralogical composition (XRPD) of precursors LOCtq, LOC700, and MA57.

Chemical Composition (wt%)			Mineralogical Composition (wt%) [c]			
	LOCtq	MA57 [b]		LOCtq	LOC700	MA57 [b]
SiO_2	29.16	42.06	Quartz [SiO_2]	4.2 (±0.3)	4.5 (±0.6)	20.8 (±1.5)
TiO_2	0.27	0.70	Kaolinite [$Al_2Si_2O_5(OH)_4$]	5.6 (±0.9)		
Al_2O_3	32.30	12.93	Illite [$KAl_2Si_4O_{10}(OH)_2$]	23.1 (±3.0)	11.5 (±2.7)	20.3 (±2.4)
Fe_2O_3	3.00	8.95	Calcite [$CaCO_3$]	5.0 (±0.6)	0.4 (±0.3)	8.5 (±0.6)
MnO	0.15	0.20	Plagioclase [$(Ca,Na)Al_2Si_2O_8$]	4.1 (±0.6)	2.6 (±0.9)	5.2 (±0.8)
MgO	0.9	2.18	Feldspar [$KAlSi_3O_8$]	1.1 (±0.3)	0.7 (±0.3)	3.1 (±0.7)
CaO	4.42	27.01	Ematite [Al_2O3]			1.2 (±0.4)
Na_2O	0.17	0.36	Amorphous	56.9 (±3.9)	80.4 (±3.3)	41.0 (±4.4)
K_2O	0.90	2.20				
P_2O_5	0.21	0.09				
L.o.I. [a]	28.51	3.31				
$SiO_2 + Al_2O_3$	61.46	54.99				
SiO_2/Al_2O_3 molar ratio	1.53	5.52				

[a] L.o.I.: weight loss after calcination at 1000 °C. [b] Data from D'Elia et al., 2023 [22]. [c] Phase quantifications were carried out by means of Rietveld refinement. Standard deviation (3σ) in parentheses.

LOCtq is characterized by a total $SiO_2 + Al_2O_3$ content of ~60 wt% and a loss on ignition of 28.5 wt%, almost similar to previously investigated sludge from the same site [41], but with a higher SiO_2/Al_2O_3 molar ratio (i.e., ~1.5, the previous one ~1). This molar ratio is lower than that of around 3–4 generally considered suitable for obtaining durable and resistant clay-based geopolymers [50], but the previous study using the same Apulian WPS [41] showed that a SiO_2/Al_2O_3 molar ratio between 1–2 can be enough to promote the alkali activation of this type of waste. Good results in terms of mechanical strength were also obtained in several previous studies for binders prepared from WPS with similar [51], or slightly higher, SiO_2/Al_2O_3 molar ratios [32,36].

It is worth noting that the WPS used here had a slightly different composition from samples from the same locality (Figure 1) used in previous experiments [41]. It can be related to the compositional variability of this type of waste, which is mainly due to environmental and productive factors, as well explained in the Section 1, thus representing

a potential limit for its reuse in large-scale productions. Hence, it would be necessary to arrange a systematic characterization, which may confirm the exact composition of the sludge at any time within each site to guarantee their recycling [40,42].

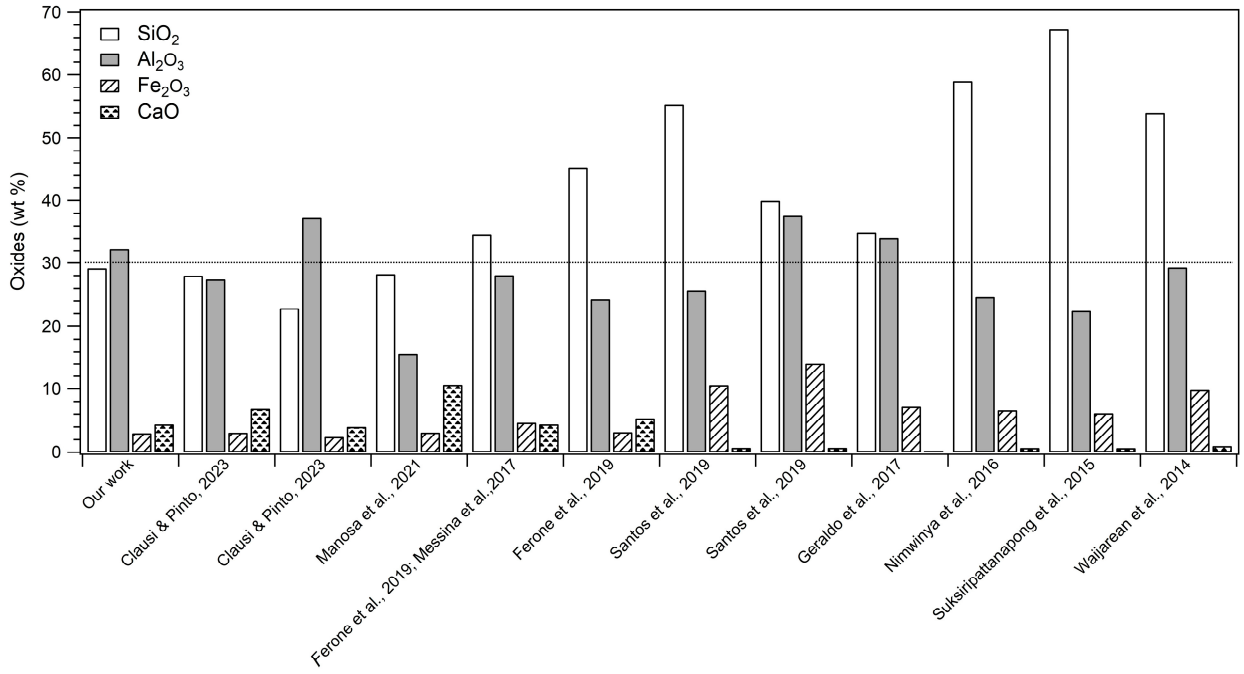

Figure 1. Percentage (wt%) of major oxides characterising WPS of previous studies [31–37,41,51].

The crystalline phases detected by XRPD in the clay precursor MA57 are quartz, illite/muscovite, calcite, and plagioclases (albite and anorthite) (Table 1). The as-is sludge (LOCtq) showed illite, kaolinite, quartz, calcite, and plagioclase as main phases. In addition, the raising of the background and the broad hump at about 20°–35° 2θ (see the diffractograms in Figure 2) indicates the presence of amorphous or low-crystalline phases that are mainly Al-based [41] and quantified as 56.9 (±3.9) wt% by the combined Rietveld-RIR method (Table 1). After the thermal treatment at 700 °C (LOC700), the reflections of kaolinite and calcite disappear and an increase in the amount of the amorphous phase is observed (80.4 (±3.3) wt%).

Granulometric analyses of the treated clay precursor (MA57) have a distribution ranging between 0.2 µm and 45 µm, with a maximum at around 3.5 µm and a shoulder at about 15 µm (Figure 3). The WPS precursors (samples LOCtq and LOC700) showed a similar multimodal distribution (ranging between 0.3 µm and 110 µm) characterized by three maxima, two of them at around 0.6 µm and 25 µm in both samples, a wider at 4 µm in LOCtq and a maximum at 2.75 µm in LOC700. As a whole, particle size distributions d50 and d90 in samples were 4 µm and 16.5 µm, respectively, in MA57, 16.4 µm and 51.8 µm in LOCtq, and 12.7 µm and 45.6 µm in LOC700. According to cumulative curves, the grain size particles of both precursors are suitable for promoting the development of well-reacted alkali-activated pastes. It is a known fact that the particle size of the precursor is one of the main factors affecting the properties of resulting alkali-activated aluminosilicates, due to its impact on the dissolution extent and, thus, on the degree of reaction and that good performances can be ensured if 80 wt% of the particle grain size is smaller than 45 µm [52,53].

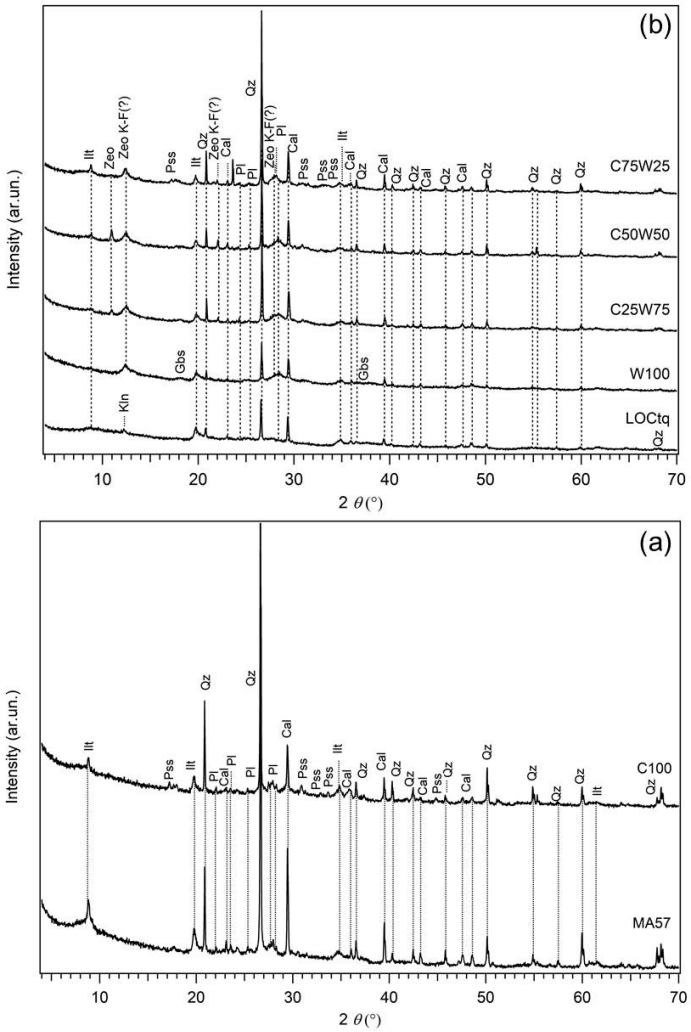

Figure 2. XRPD patterns of AABs: (**a**) MA57 clay and C100 sample, (**b**) LOCtq and LOCtq-based samples. Sample labels are on top of each pattern. Precursors MA57 and LOCtq are reported as references in the bottom of images. Cal = Calcite; Gbs = gibbsite; Ilt = Illite; Kln = Kaolinite; Pl = Plagioclase; Pss = pirssonite; Qz = Quartz; Zeo = zeolitic phase of uncertain attribution; Zeo K-F = zeolite K-F.

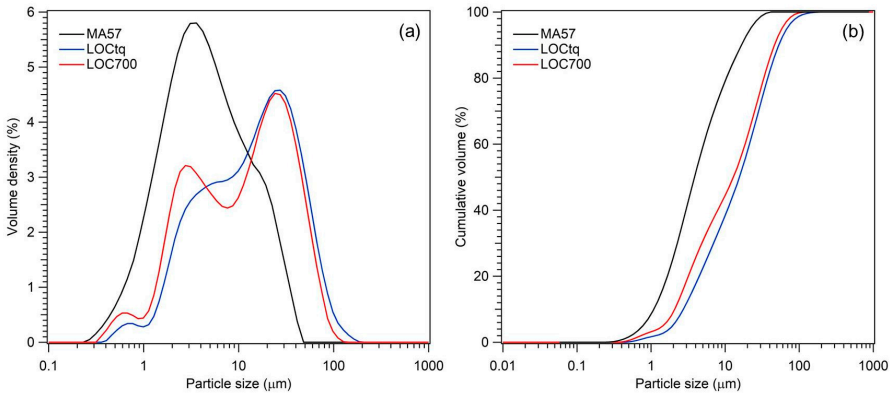

Figure 3. Grain-size distributions (**a**) and cumulative percentage volumes (**b**) of MA57 (black line), LOCtq (blue line), and LOC700 (red line).

3.2. Characterization of Alkali-Activated Blends

A total of eight different samples (Table 2) were prepared by mixing the clay (MA57) with the untreated WPS sludge (LOCtq) and the heated sludge (LOC700) in different proportions and cured in environmental conditions during summer season, under very hot external temperatures (more than 35 °C). To evaluate the influence of external environmental conditions on the experiments, a second set of samples was prepared during the winter season under temperatures (T °C) and relative humidities (R.H.) completely different from those of the first set of samples. This second group (four samples) only included the blends of the clay with the heat-treaded sludge (MA57-LOC700) as they showed better characteristics according to the first synthesis experiment (see following discussions). A summary is reported in Table 2 together with results of compressive strength and chemical stability tests (discussed in Sections 3.2.2 and 3.2.3, respectively).

Table 2. Details of AABs.

Environmental conditions		Samples Label	Precursors Weight Ratio			S/P [2]	Compressive Strength (MPa)	Integrity Test (24 h)	Stability Test (10 d)
			MA57	LOCtq	LOC700				
	(ss) T °C ≥ 35 °C; RH ≥ 65%	C100	100	0	0	0.56 [3]	16 (4)	✔	✔
		C75W25	75	25	0	0.8	4.1 (3)	✔ [4]	✔✘ [6]
		C50W50	50	50	0	0.8	5.6 (1.5)	✘ [5]	// [7]
		C25W75	25	75	0	0.8	4.5 (1)	✘	//
		W100	0	100	0	0.85	//	✘	//
		C75WT25s [1]	75	0	25	0.95	3.8 (5)	✔	✔
		C50WT50s	50	0	50	0.95	2.9 (2)	✔	✔
		C25WT75s	25	0	75	0.95	4.9 (7)	✔	✔
		WT100s	0	0	100	1	7.1 (4)	✔	✔
	(ws) 10 °C < T °C < 20 °C; RH ~50%	C75WT25w [1]	75	0	25	0.95	7.5 (1)	✔	✔
		C50WT50w	50	0	50	0.95	4.4 (3)	✔	✔
		C25WT75w	25	0	75	0.95	7.3 (1.3)	✔	✔
		WT100w	0	0	100	1	9.2 (8)	✔	✔

[1] s or w differ samples by curing environment. [2] S/P = alkali solution/precursor weight ratio. [3] S/P used in D'Elia et al., 2023 [22]. [4] ✔ = No crack. [5] ✘ = Fragmentation. [6] ✔✘ = some crack. [7] // = test not performed.

3.2.1. Mineralogical and Microstructural Properties of the Hardened Pastes

The XRPD pattern of the hardened pastes at the 28th curing day are presented in Figures 2 and 4 in comparison with that of each solid precursor. The sample prepared using the single clay precursor (sample C100) had a slight hump located about 2θ = 25–40°, characteristic of the low structural order phase related to the alkali activation reaction. Among the crystalline phases, pirssonite [$Na_2Ca_2(CO_3)_2$ $2H_2O$], a calcium sodium carbonate commonly found in alkali-activated materials derived from the Ca-rich precursors [54], was detected in addition to the clay quartz, illite, calcite, and feldspars already occurring in the clay (Figure 2a). However, the X-ray intensities of calcite and illite appear lower in the hardened pastes, suggesting a certain degree of their reaction during the alkali activation.

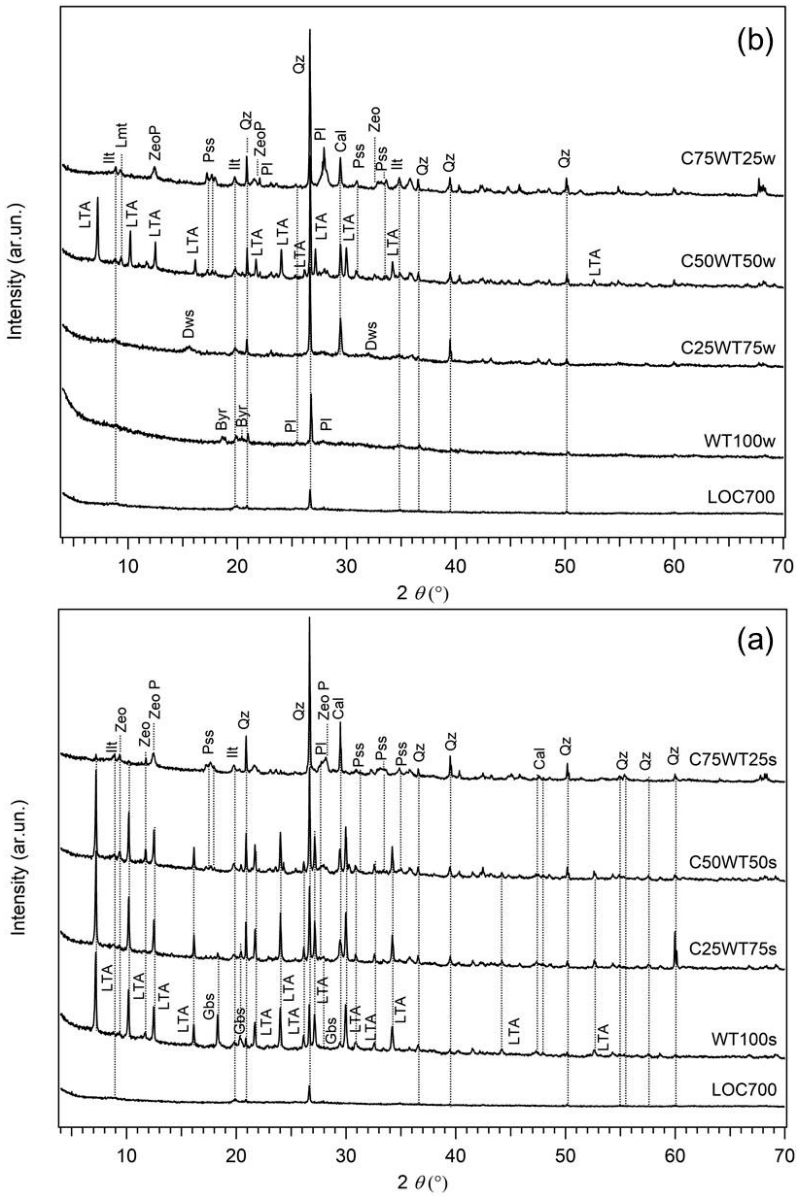

Figure 4. XRPD patterns of AABs: (**a**) LOC700-based samples cured in summer season, (**b**) LOC700-based samples cured in winter season. Samples labels are on top of each pattern. Precursor LOC700 is reported as reference in the bottom of images. Byr = bayerite; Cal = Calcite; Dws = Dawsonite; Gbs = gibbsite; Ilt = Illite; Kln = Kaolinite; Lmt = Laumontite; LTA = zeolite LTA; Pl = Plagioclase; Pss = pirssonite; Qz = Quartz; Zeo = zeolitic phase of uncertain attribution; ZeoP = zeolite P.

In samples prepared from the replacement of the clay with the untreated sludge (LOCtq) (Figure 2b) the same crystalline phases from the clay are observed with amounts proportional to the clay content. Besides, several X-ray reflections of newly formed phases are also present. Specifically, two main wide reflections from ~10 to ~16 2ϑ and from ~24 to ~32 2ϑ were observed in the diffraction patterns of all the samples and explained by the incipient formation of a zeolitic phase, presumably attributable to Na-exchanged zeolite K-F type (PDF 39–217) [55]. The occurrence of this zeolite type has been recently found in low-Si metakaolin-based geopolymers synthesised for Cs immobilization [56]. Instead, in the clay-rich blend (sample C75W25), the occurrence of pirssonite isdetected in XRPD data. The formation of this phase is related to the Ca content from the clay, as said above. A further peak of about d = 8.05 Å of uncertain attribution is also present in the X-ray diffraction patterns of the blends. Although, any reliable attribution could be

performed based on the available data, it can be tentatively ascribed to a zeolitic phase, i.e., a sodium aluminium silicate zeolite of type Nu-3 zeolite (PDF 47–705) or ZSM-25 zeolite (PDF 43–24). It is worth noting that the intensity of this peak increases in WPS-rich samples, but the peak is not present in the samples prepared from the single precursors alone. This suggests that it is related to a phase whose formation is influenced by the sludge content, but only in the case of blends with the clay, probably due to the higher availability of silicon. Therefore, this phase does not form in W100 (containing 100% of LOCtq precursor), where the aluminium hydroxide gibbsite can crystallize as separate phase instead, owing to the high content of Al present from the sludge with react with OH^- in solution [41].

When considering samples prepared by replacing the clay (MA57) with WPS heated to 700 °C (LOC700) and cured during the summer season (Figure 4a), it was shown that zeolite LTA [$Na_{12}Al_{l2}Si_{12}O_{48}$ $(H_2O)_{27}$] occurs as main newly formed crystalline phases in samples with more than 50% of sludge (C25WT75s, C50WT50s), suggesting that the formation of this zeolite type is favoured when sludge content is 50% or higher. Further crystalline phases are gibbsite [$Al(OH)_3$] and pirssonite, the former being present principally in sludge-rich samples (WT100s and C25WT75s), the latter in clay-rich samples (C50WT50s, C75WT25s). Two additional small reflections at d = 9.44 Å and d = 7.50 Å were also observed in all the samples, which may tentatively be assigned to other zeolitic phases having principal X-ray reflections in those positions (i.e., laumontite, PDF 47–1785, or chabazite, PDF 53–1177, for the reflection with d = 9.44 Å, zeolite ZK-5, PDF 37–360, for that with d = 7.50 Å). However, the very low intensities of the observed peaks and the absence of any other diffraction reflections do not permit a univocal assignment. In the sample with a 25% clay-for-sludge substitution (C75WT25s) zeolite LTA is lacking (or present only as traces), whereas zeolite P [$Na_6Al_6Si_{10}O_{32}(H_2O)_{12}$] occurs as new phase together with pirssonite, in addition to the other phases from the clay (quartz, calcite, plagioclase, K-feldspar, and illite).

The comparison with the corresponding samples cured under different atmospheric conditions (i.e., the winter season with external temperature from 10 °C to 20 °C) clearly shows out that, in the case of the sample with only the sludge or with 75% of it (WT100w and C25WT75w, respectively), no LTA zeolite is formed, but bayerite [$Al(OH)_3$] and dawsonite, a hydroxycarbonate of sodium and aluminium with formula [$NaAl(CO_3)(OH)_2$)], are, respectively formed as secondary phases (Figure 4b). The occurrence of these Al hydroxides is due to the large availability of aluminium from the sludge reacting with OH^- in solution [41]. The absence of any other crystalline phases (except for those from the clay) indicates the presence of a more extended amorphous phase in the samples cured under colder atmospheric condition with respect to those under warmer temperatures. In samples with higher content of the clay, no significant compositional difference is observed at the two curing conditions, but while in 50:50 LOC700/clay samples (C50WT50s and C50WT50w), zeolite LTA is the main phase formed, in the samples with 75% of clay and 25% of LOC700 (C75WT25s and C75WT25w, respectively) only limited amounts of zeolite P and laumontite [$Ca_4Al_8Si_{16}O_{48}16H_2O$], together with pirssonite, are detected in the XRPD data (Figure 4). No comprehensive explanation can be given to this evidence, but it can be tentatively related to the different content of reactive silicon and then Si/Al ratio in the two systems. In the former case, the availability of Si from the clay is too low for the extended formation of the amorphous phase, but enough to prevent the formation of a separate hydroxide, so zeolite LTA could form, independently by the curing conditions. In the second case, the higher amount of Si from the clay favours the formation of the amorphous in addition to minor zeolite P, which has higher Si/Al ratio than zeolite LTA.

At the microscopic scale (Figure 5a), a brownish paste, in which different sized particles can be distinguished, characterizes C100 sample. Similarly, blend samples (Figure 6) are characterized by a grey-coloured paste and brownish aggregates of variable size and shape. The amount of these particles is greater in samples containing 75% or 50% of the clay precursor, leading to the assumption that they are related to a certain amount of clay fraction that did not undergo the reaction. Furthermore, the presence of these clusters seems to produce discontinuity in the matrices, independently from the type of mixture.

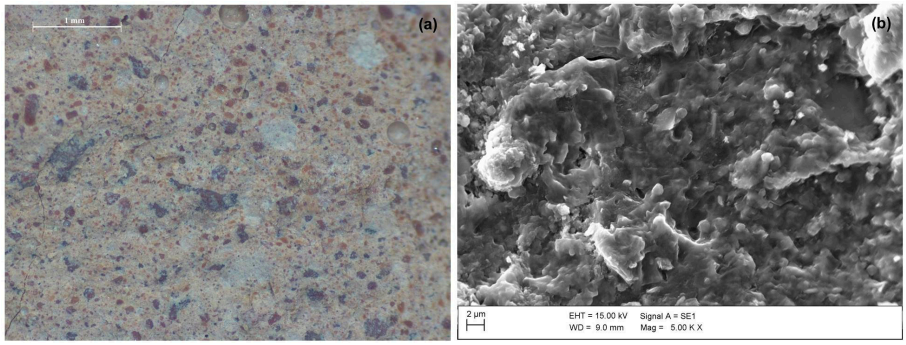

Figure 5. (**a**) Stereomicroscopic image at magnification 20× (scale bar of 1 mm) and (**b**) SEM micrograph at magnification 5 Kx of C100 sample.

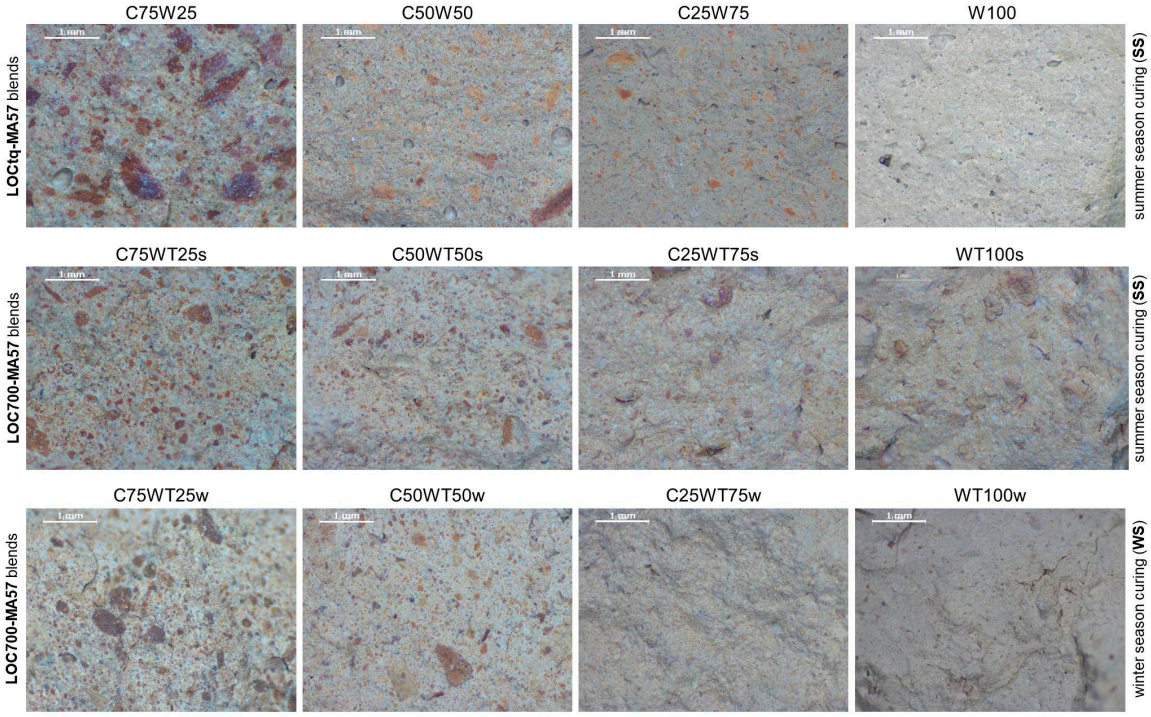

Figure 6. Stereomicroscopic images (magnification 20×—scale bar of 1 mm in the figures) of inner sections of AABs. Each line refers to a type of blend (reported on the left of the line); the season of year in which samples were cured (summer (ss) or winter (ws)) is reported on the right of the line; sample names are reported on the top of each image.

Anyway, the substitution of untreated sludge (LOCtq) or heated sludge (LOC700) to the clay (MA57) leads to quite different microstructures compared to that mainly amorphous and bonded of C100 sample (Figure 5b), as can be observed from SEM micro photos in Figure 7. LOCtq-MA57 blends show matrices constituted by partially bonded particles, in which the morphology of unreacted phases from the precursors (e.g., the elongated phyllosilicates morphology) were recognized. Micrographs of LOC700-MA57 blends show almost granular microstructures constituted mostly by clusters of crystal nuclei less than 1 µm in size. From their crystal shape, similar to zeolite LTA [28,57] and their SiO_2/Al_2O_3 ratio at around 2, as measured by the EDX analyses (Figure 8). The observed crystal clusters can be identified as zeolite LTA, in agreement with results from XRPD analyses.

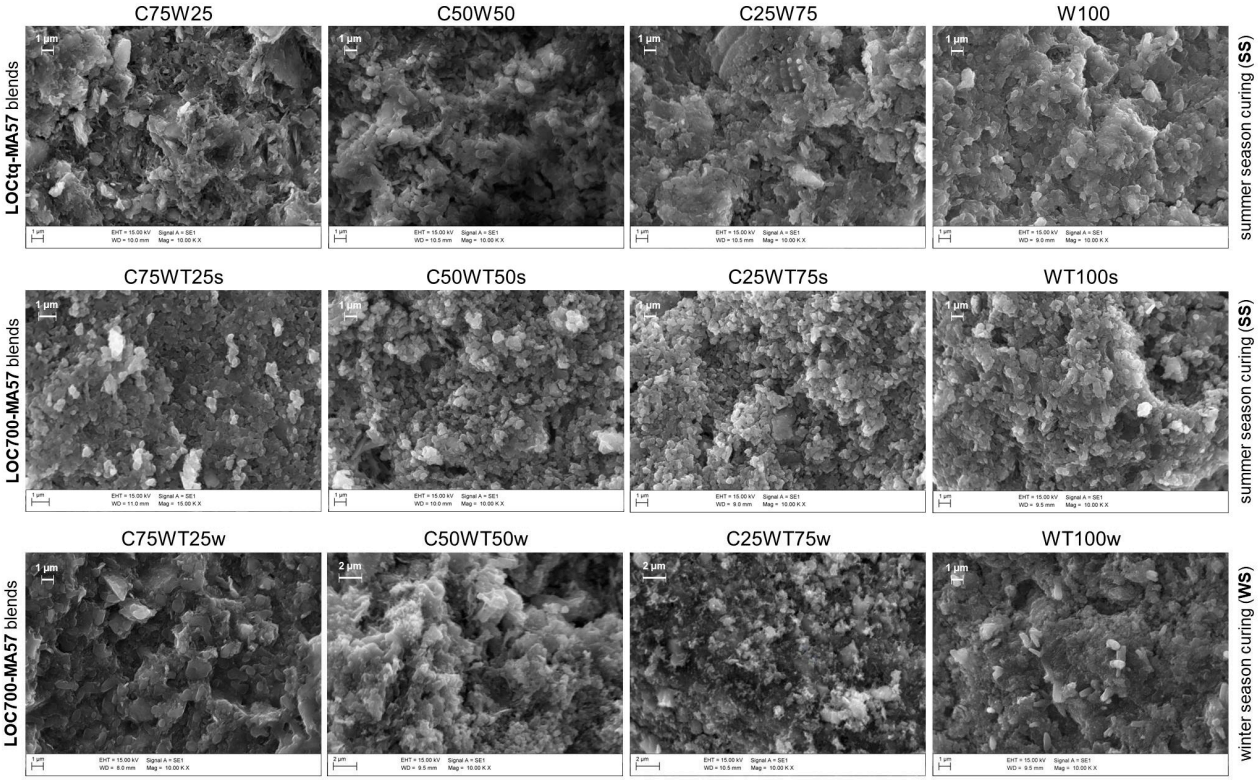

Figure 7. SEM micrographs of AABs. Each line refers to a type of blend (reported on the left of the line) the season of year in which samples were cured (summer (ss) or winter (ws)) is reported on the right of the line. The sample names are reported on the top of each image. Scale bar and magnification are shown both on the top of images and in the informative boxes at the bottom of them.

The microstructures of samples prepared during the winter season (Figure 6) appear poorer of crystalline aggregates, conversely to those prepared during the summer, suggesting a more extended development of an amorphous matrix, with compactness growing by increasing LOC700 amount. However, in agreement with the XRPD findings, different crystals are also recognizable in the matrices, as those clearly evident in Figure 8.

3.2.2. Mechanical Strengths

The mechanical test results are reported in Table 2. The C100 sample (prepared using the sole clay precursor) provided mechanical strength of 16 MPa, consistent with previous findings [21,22]. The substitution of clay with the as-is sludge (LOCtq) significantly decreased the mechanical strengths of the samples to around 4 MPa, independently from the mixture proportions. Furthermore, samples with 100% of LOCtq (W100) showed a premature failure before the end of the 28-d curing time, by developing diffuse creaking, so no compressing strength data could be measured for W100 despite samples were prepared twice. However, the results obtained using the uncalcined sludge are almost comparable with literature findings on similar systems, as can be observed in Table 3. Compressing strength from 1.3 to 3.4 MPa were obtained for alkali-activated pastes which were prepared using untreated WPS and non-dehydroxylated kaolinitic clay, NaOH as activating solution, and a curing temperature of 80 °C [31]. Similarly, only 0.76 MPa were obtained for samples prepared using uncalcined sludge and NaOH by Waijarean and co-workers [36] after 60 days of curing at 28 °C. They attributed this low value to the low amorphous content of the precursor related to the non-dehydroxylation of the aluminosilicate source, but it is our opinion that the high occurrence of organic matter in uncalcined WPS have a significant role in reducing the binder capacity of the paste and the development of the alkali activation reaction, thus explaining the premature cracking in sample W100 and also the results of solubility test in water (see the following paragraph).

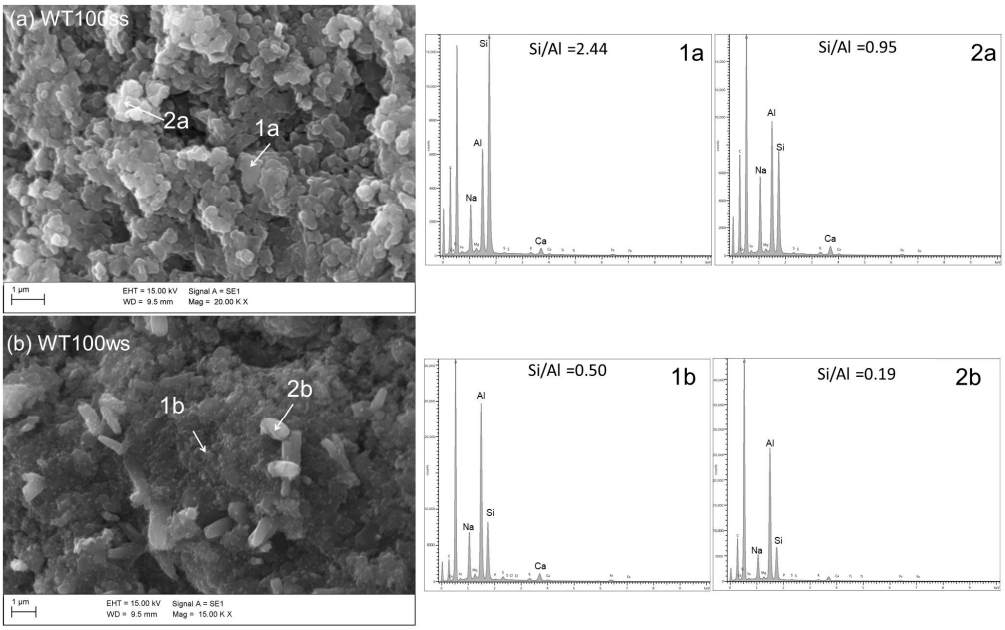

Figure 8. SEM micrographs and EDX analyses of samples (**a**) WT100ss and (**b**) WT100ws. Scale bars and magnifications are shown in the images.

Table 3. Summary of characteristics of AABs produced by using WPS or WPS/clay as precursors.

	Precursors	WPS Pre-Treatment (°C)	Alkaline Activator	Curing Design	Compressive Strength (MPa) [d]
Our work	WPS	no, 700	NaOH	RT °C	0–9.2
Ferone et al., 2019 [32]	WPS	650	SS [b]	25 and 60 °C for 7 days than RT °C	3.9–15.2
Nimwinya et al., 2016 [35]	WPS	600	NaOH + SS	27–30 and 60 °C for 7 days than RT °C for 24 h	~5–7
Waijarean et al., 2014 [36]	WPS	no, 600, 800, 900	NaOH	28 °C until 60 days	0.76–~8.5
Our work	WPS (25–50–75%) [a]–clay	no, 700	NaOH	RT °C	2.9–7.5
Manosa et al., 2021 [31]	WPS (5–10–20–40–80%)—clay	no	NaOH	80 °C for 24 h then RT °C for 14 days	~1.3–3.4
Messina et al., 2017 [34]	WPS (30–50–70%)—clay sediments	750	NaOH + SS	20 and 60 °C for 24 h than 20 °C, RH > 90% and RT °C	18–23
Geraldo et al., 2017 [33]	WPS (15–30–60%)—metakaolin (+sand)	no	NaOH + RHA [c]	25 °C, RH = 60%	9–~25

[a] In parenthesis the amount of WPS substituted to clay. [b] SS = Sodium silicate solution. [c] RHA = rice husk ash. [d] Compressive strength measured between 7 and 60 days.

The calcination of WPS at 700 °C significantly improves the compressive strengths of the samples prepared from the sole sludge (WT100s and WT100w), although a difference is observed for samples cured under different environmental conditions, with winter samples showing higher compressive strengths than the summer ones (~9 MPa and 7 MPa, respectively). Anyway, the obtained strength values are generally in agreement with those in the study by Waijarean et al. [36], whereas WPS was calcined at 800 °C (~8.5 MPa) and with results from the studies of Nimwinya et al. [35] and Ferone et al. [32], which are summarized in Table 3. It is worth noting that in the latter two studies a calcination temperature of about 600 °C was selected and sodium silicate solutions were used

as an activator, but better or almost similar compressive strengths were only obtained for samples after curing at 60 °C, while near environmental curing conditions gave lower compressive strengths (Table 3). According to Ferone et al. [32], curing at 60 °C promotes the development of micro fractures in the samples.

The blends of LOC700 and MA57 clay show generally lower compressive strengths than the two precursors alone, indicating a bad interaction between the two precursors, at least under the selected experimental conditions (only NaOH as activator and room temperature curing). Furthermore, worse strength values are generally observed for samples cured in warmer environmental conditions (summer season) than those prepared during the winter, analogous to the samples from the pure calcinated WPS. It can be explained by the higher content of zeolite developed in the former set of samples, which reduced the binder capacity of the samples, as also indicated by the general development of micro fractures in these samples (Figure 9). Similar evidence is described in Ferone et al. [32] for samples cured at 60 °C. Analogously, the authors explain the lower mechanical strengths of the blends 50:50 (C50WT50s and C50WT50w), showing higher amounts of zeolite LTA. The crystallization of this type of zeolite was also found in Ferone et al. [32], who attributed its occurrence to the combination of a low Si/Al ratio of the systems with the curing at temperature (60 °C).

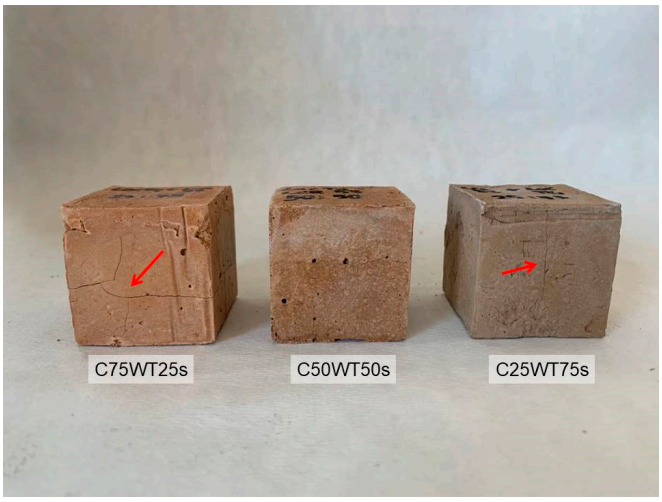

Figure 9. Micro fractures (evidenced by arrows) in some samples cured during the summer season.

From the comparison of our results with mortars obtained from blends of similar WPS clay sediments and sand, but using sodium silicate as alkaline activator [34], a significant improvement of mechanical strengths is evident, both under low temperature curing and at 60 °C (Table 3), suggesting the necessity of the integration of a silicon source in such a system to develop well-hardened pastes. The integration with a silicon source, i.e., rice husk ash, has also been tested in the study of Geraldo et al. [33], who obtained well-hardened mortars from the admixture in different amounts of uncalcined WPS with metakaolin and sand (Table 3).

Taking into account the results of our study and the available literature it is thus possible to conclude that mechanical strengths of hardened pastes obtained from the alkali activation of WPS are strongly influenced by the thermal pretreatment of the sludge, type of alkaline solution and curing conditions. The use of the sole non-calcinated WTS for the alkaline activation process is generally not recommended, but generally better compressive strengths can be obtained when WTS is admixed with clay. Instead, the calcination of WTS at a temperature of at least 700 °C significantly improves the mechanical properties the hardened pastes obtained both using WTS as unique precursor or in combination with clay. Furthermore, our study demonstrated that the use of NaOH solutions for the alkaline activation of WTS can promote the formation of well-hardened pastes with compressive

strengths almost similar to those obtained using sodium silicate alkaline activations, therefore significantly reducing the carbon footprint of the process. The addition of a further silica source would be desirable to balance the high Al content of the WTS in order to increase the Si/Al ratio, therefore improving the mechanical properties of the hardened pastes and, at the same time, avoiding the formation of secondary hydroxides. To this aim, the use of rice husk ash seems to be a good option, particularly when admixed with metakaolin. Carbonate-rich clays showed generally low compatibility with WTS as their admixture in all the proportions gave worse strengths than the single precursors alone. However, it is the authors' opinion that it could be related to the experimental choice of environmental curing, so better results could be expected by the curing of pastes under more controlled conditions or higher temperatures, as also inferred from the literature data summarised in Table 3. A similar conclusion was also drawn by D'Elia et al. [22] for a blend of the same clay, MA57 with fly ash, which produced pastes with mechanical strengths lower than that of the single precursors and showed presence of unreacted fly ash, so suggesting to necessity to improve the reaction of precursors by modifying the curing parameters.

However, the evidence of very different reaction products in the samples prepared under different environmental conditions further suggest the necessity of curing under more controlled temperatures for the investigated blends here to allow for the reproducibility of the synthesis procedure and results.

Owing to the above statements, it is possible to assert that the blends investigated here cannot be addressed in terms of site-poured applications, but rather for precast building materials (i.e., blocks, panels, and brick) whose compressive strengths may range from 6–10 MPa (e.g., for bricks) to a minimum of about 30 MPa in the case of precast concrete. The results obtained from this study are thus encouraging and evidence several optimization roots in the preparation of the mixes and in curing conditions which can be addressed to improve the properties of the final materials and make their synthesis more sustainable. In a recent paper by Messina and co-workers [34], precast paving cement-free bricks were upscaled by the optimization of mixes obtained by the synergic recycling of calcined clayey sediments and WPS. However, the use of sodium silicate as an activating solution reduced the ecological footprint resulting from the use of wastes as raw materials significantly. In contrast, our study opens to the possibility to obtain well-hardened pastes from the alkaline activation of WPS, but using only NaOH as activating solution, although with a better control of curing parameters.

3.2.3. Chemical Stability of Products in Water

Integrity tests were conducted to obtain a direct feedback on the stability of the alkali-activated products in water, since water leads to disaggregate the structure if the reaction is non-fully occurred [49]. Test results have been evaluated through direct observations, considering both water clarity and samples fragmentation (Figure 10). All the samples prepared using the uncalcined WPS, except for C75W25, showed damaged surfaces after 24 h, suggesting that the maximum percentage of WPS for clay substitution to obtain an acceptable binder without the thermal pre-treatment of the sludge is around 25%. This result is in agreement with Manosa et al. [31], who found that samples containing more than 20% of WPS failed chemical stability tests. Conversely, all samples of the LOC700-MA57 series passed integrity tests (Table 2), showing undamaged surfaces after 24 h. The longer soaking time of 10 days did not influence the chemical stability in the water of these samples, testifying for the development of well reacted pastes.

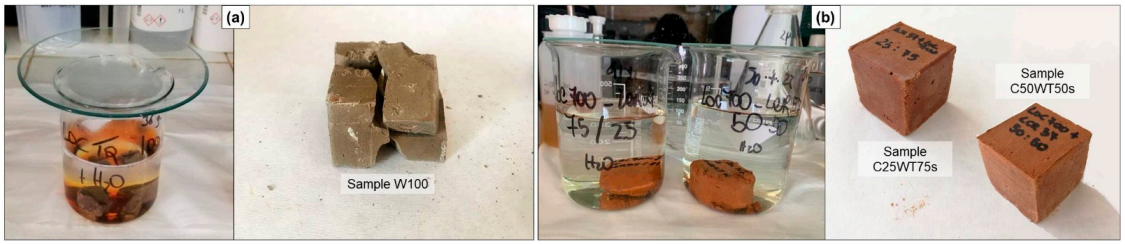

Figure 10. Appearance of the alkali-activated samples during and after soaking in water for 10 days: (**a**) W100 sample; and (**b**) C50WT50s and C25WT75s samples.

4. Conclusions

In this work, alkali activated blends were synthesized from water potabilization sludge (WPS) and a natural clay sourced in the same territory (Apulian region, South Italy), with the aim of verifying the compatibility between the two precursors and the partial and/or entire replacement of a natural and finite clay resource with an unavoidable waste, produced by a current water potabilization process. To this purpose, firstly two sets of materials were made, using raw and thermally activated sludge, respectively, by gradually increasing the sludge percentage of 25% in substitution of clay, until to obtain an exclusively waste-derived binder. In the perspective of more sustainable processes, sodium hydroxide solutions, commonly considered less polluting than other types of activators, and room temperature curing conditions were used. Samples were prepared in a different period of the year, to verify the influence of uncontrolled room temperature curing conditions on physicochemical features of hardened pastes.

From the results of this study, the authors evidenced a lacking interaction between the two selected precursors, i.e., MA57 clay and WPS, either when using untreated WPS or after its heating to 700 °C. Unreacted clay fractions were revealed in the matrices, showing that the species involved in alkali activation did not guarantee enough aluminosilicate gel formation, which explained the mechanical strength differences of the blends compared to the hardened paste with the sole clay (sample C100). Furthermore, the role of untreated (LOCtq) and heat-treated sludge (LOC700) in the blends was found to be different. LOC700 played an active role in the alkali activation of the blends (enriching gels in amorphous Si, Al, and Ca). However, the strength values of the mixes were influenced by the formation of crystalline phases rather than the development of aluminosilicate gel. The clay-for-sludge substitution did not positively affect the technical characteristics of the hardened pastes and indeed, among the tested samples, the highest mechanical strength values were recorded for those with single precursors alone. Limited to the conditions applied in this study, this means that although it is possible to replace clay with calcined WPS in percentages of up to 75%, the mechanical strength values were strongly influenced not only by the percentage of sludge substitution in the blends but also to the environmental conditions (T °C and RH%) in which the samples were matured. Samples cured under different temperature environments produced quite different productsin particular for the percentage of LOC700 substitution greater than 50%: well-crystallized zeolite-LTA type formed during curing in summer temperature conditions, whereas mostly amorphous matrices, together with traces of the Al-bearing hydroxides bayerite ($Al(OH)_3$) and dawsonite ($(NaAl(CO_3)(OH)_2$), were produced in samples cured under colder winter temperatures. A significant decrease of mechanical strength was observed in samples with extensive crystallizations of zeolite. Instead, in the samples with a LOC700/MA57 clay ratio equals to 1:3 and 1:1, a limited amount of low crystalline zeolite P, in addition to amorphous phase, and well crystallized zeolite LTA formed, respectively, almost independently to the curing conditions. No exhaustive explanation could be given for this different behaviour, but it has been attributed to the higher availability of silicon apported to the system by increasing the content of clay in the blends, which allowed the formation of an amorphous gel and, secondarily, a zeolite phase with Si/Al = 3, only in the sample with 75% of clay.

In the case of the untreated WPS (LOCtq), its involvement in alkali activation was found to be limited as the sludge acted mainly like a filler, contributing to compact the matrices. Furthermore, it can be said that the use of the untreated WPS showed some criticalities probably due to its high content of organic matter, so the blends containing more than 25% of the sludge failed the integrity test.

Overall, the compressive strength results obtained in this study for the tested mix designs are encouraging. Such strength values are too low if compared to those of traditional binders and mortars, but they can be considered encouraging in the perspective of applications for non-structural precast materials. This conclusion is further confirmed by the strong difference in the structure and properties of samples obtained under different seasonal climatic conditions, which clearly suggest that the uncontrolled environmental temperature is not an optimal curing method. Hence, future research on WPS/clay under different temperatures and/or more controlled curing conditions are desirable ss assuring more sample replicability, but at the same time for optimizing the physical and chemical properties of the hardened pastes, also in the perspective of further broader application fields. In this connection, an interesting perspective is represented by the possibility of addressing synthesis parameters to develop geopolymer–zeolite composites with specific properties for their applications as bulk-type adsorbents and membranes. Such hybrid aluminosilicate systems are still poorly investigated, but promising adsorbent materials characterized by an inter-connected multiscale distribution of pores as they combine the intrinsec properties of the geopolymeric meso- and macro-porous matrix, acting as a strong and durable support for zeolites, and the microporosity of zeolites providing high surface area, porosity and adsorption capacity [58]. The results obtained in this study about the conditions controlling the development of cristalline zeolite and geopolymeric amorphous matrix in clay-WPT blends contributed to the field of these hybrid aluminosilicate materials, in particular demonstrating the possibility of also synthetizing them at room temperature.

By summarizing the main results of this study, it is possible to highlight the following points:

- Alkaline activation of WPS in blends with clay can be an effective strategy to convert a waste, usually destined to landfill, into value-added products, so resulting into eco-sustainable and economic processes, considering that it is a widely and locally available industrial by-product.
- In the case of mixes with uncalcined WPS the optimal formulation was reached with 25 wt% WPS, as it gave the highest compressive strengths and best chemical stability. The calcined WPS can be substituted up to 75%, but a substitution of about 25% is more suitable in the case of environmental conditions as it resulted in less dependence on the curing conditions.
- The use NaOH in the alkaline activation of WPS can promote the formation of well hardened pastes, so it should be preferred to the more expensive and less sustainable sodium silicate.
- The necessity of better control of the curing conditions of the blends emerges from this study in order to improve the properties of the hardened pastes and assure the reproducibility of results.
- This study showed that different kinds of hybrid geopolymer-zeolite systems can be obtained at varied environmental curing temperatures, so offering interesting insights in the field of these composites as sorbent materials.

Author Contributions: Conceptualization, M.C. and D.P.; Methodology, M.C. and D.P.; Validation, M.C. and D.P.; Formal analysis, G.G., M.C. and D.P.; Investigation, M.C. and D.P.; Data curation, M.C. and D.P.; writing—original draft preparation, G.G., M.C. and D.P.; writing—review and editing, M.C. and D.P.; Visualization, M.C.; Supervision, D.P.; Project administration, D.P.; Funding acquisition, D.P. All authors have read and agreed to the published version of the manuscript.

Funding: The research was financially supported by POR Puglia 2014/2020-Asse X-Azione 10.4 Research for Innovation (REFIN) (grant 93E5DCB6) and by University of Bari Aldo Moro through the fund Next Generation EU-MUR D.M. 737/2021 (grant S64-H91I21001710006-Horizon Europe Seeds).

Institutional Review Board Statement: Not applicable.

Informed Consent Statement: Not applicable.

Data Availability Statement: Further inquiries can be directed to the corresponding author.

Acknowledgments: The authors would like to thank: Acquedotto Pugliese S.p.a. for providing materials; Tecno-Lab s.r.l for assisting in mechanical test; laboratory technicians M. Pallara R. Vittoria and N. Mongelli for their help during the laboratory analyses. This work benefited from instrumental upgrades of Potenziamento Strutturale PONa3_00369 degli Studi di Bari "A. Moro" entitled "Laboratorio per lo Sviluppo Integrato delle Scienze e delle TEcnologie dei Materiali Avanzati e per dispositivi innovativi (SISTEMA)".

Conflicts of Interest: The authors declare no conflict of interest.

References

1. Palomo, A.; Maltseva, O.; Garcia-Lodeiro, I.; Fernández-Jiménez, A.; Leonelli, C.; Mackenzie, K.J. Portland Versus Alkaline Cement: Continuity or Clean Break: "A Key Decision for Global Sustainability". *Front. Chem.* **2021**, *9*, 705475. [CrossRef]
2. Shi, C.; Jiménez, A.F.; Palomo, A. New Cements for the 21st Century: The Pursuit of an Alternative to Portland Cement. *Cem. Concr. Res.* **2011**, *41*, 750–763. [CrossRef]
3. Pacheco-Torgal, F.; Castro-Gomes, J.; Jalali, S. Alkali-Activated Binders: A Review. Part 2. About Materials and Binders Manufacture. *Constr. Build. Mater.* **2008**, *22*, 1315–1322. [CrossRef]
4. Davidovits, J. Geopolymers. *J. Therm. Anal.* **1991**, *37*, 1633–1656. [CrossRef]
5. Duxson, P.; Provis, J.L.; Lukey, G.C.; van Deventer, J.S.J. The Role of Inorganic Polymer Technology in the Development of "Green Concrete". *Cem. Concr. Res.* **2007**, *37*, 1590–1597. [CrossRef]
6. Pacheco-Torgal, F.; Castro-Gomes, J.; Jalali, S. Alkali-Activated Binders: A Review. Part 1. Historical Background, Terminology, Reaction Mechanisms and Hydration Products. *Constr. Build. Mater.* **2008**, *22*, 1305–1314. [CrossRef]
7. Liew, Y.-M.; Heah, C.-Y.; Mohd Mustafa, A.B.; Kamarudin, H. Structure and Properties of Clay-Based Geopolymer Cements: A Review. *Prog. Mater. Sci.* **2016**, *83*, 595–629. [CrossRef]
8. Shi, C.; Qu, B.; Provis, J.L. Recent Progress in Low-Carbon Binders. *Cem. Concr. Res.* **2019**, *122*, 227–250. [CrossRef]
9. Luukkonen, T.; Heponiemi, A.; Runtti, H.; Pesonen, J.; Yliniemi, J.; Lassi, U. Application of Alkali-Activated Materials for Water and Wastewater Treatment: A Review. *Rev. Environ. Sci. Bio/Technol.* **2019**, *18*, 271–297. [CrossRef]
10. Pacheco-Torgal, F.; Labrincha, J.; Leonelli, C.; Palomo, A.; Chindaprasit, P. *Handbook of Alkali-Activated Cements, Mortars and Concretes*; Elsevier: Amsterdam, The Netherlands, 2014; ISBN 1782422889.
11. Jindal, B.B.; Alomayri, T.; Hasan, A.; Kaze, C.R. Geopolymer Concrete with Metakaolin for Sustainability: A Comprehensive Review on Raw Material's Properties, Synthesis, Performance, and Potential Application. *Environ. Sci. Pollut. Res.* **2022**, *30*, 25299–25324. [CrossRef]
12. Provis, J.L.; Yong, S.L.; Duxson, P. 5-Nanostructure/Microstructure of Metakaolin Geopolymers. In *Woodhead Publishing Series in Civil and Structural Engineering*; Provis, J.L., van Deventer, J.S.J.B.T.-G., Eds.; Woodhead Publishing: Sawston, UK, 2009; pp. 72–88; ISBN 978-1-84569-449-4.
13. Khalifa, A.Z.; Cizer, Ö.; Pontikes, Y.; Heath, A.; Patureau, P.; Bernal, S.A.; Marsh, A.T.M. Advances in Alkali-Activation of Clay Minerals. *Cem. Concr. Res.* **2020**, *132*, 106050. [CrossRef]
14. El Khomsi, A.; Ghaezouni, A.; Kandri, N.I.; Zerouale, A.; Rossignol, S. Moroccan Clays for Potential Use as Aluminosilicate Precursors for Geopolymer Synthesis. *E3S Web Conf.* **2021**, *240*, 3001. [CrossRef]
15. Valentini, L.; Contessi, S.; Dalconi, M.C.; Zorzi, F.; Garbin, E. Alkali-Activated Calcined Smectite Clay Blended with Waste Calcium Carbonate as a Low-Carbon Binder. *J. Clean. Prod.* **2018**, *184*, 41–49. [CrossRef]
16. Buchwald, A.; Hohmann, M.; Posern, K.; Brendler, E. The Suitability of Thermally Activated Illite/Smectite Clay as Raw Material for Geopolymer Binders. *Appl. Clay Sci.* **2009**, *46*, 300–304. [CrossRef]
17. Žibret, L.; Wisniewski, W.; Horvat, B.; Božič, M.; Gregorc, B.; Ducman, V. Clay Rich River Sediments Calcined into Precursors for Alkali Activated Materials. *Appl. Clay Sci.* **2023**, *234*, 106848. [CrossRef]
18. Rahman, M.M.; Law, D.W.; Patnaikuni, I.; Gunasekara, C.; Tahmasebi Yamchelou, M. Low-Grade Clay as an Alkali-Activated Material. *Appl. Sci.* **2021**, *11*, 1648. [CrossRef]
19. Valentini, L.; Moore, K.R.; Bediako, M. Sustainable Sourcing of Raw Materials for Construction: From the Earth to the Moon and Beyond. *Elements* **2022**, *18*, 327–332. [CrossRef]
20. D'Elia, A.; Pinto, D.; Eramo, G.; Giannossa, L.C.; Ventruti, G.; Laviano, R. Effects of Processing on the Mineralogy and Solubility of Carbonate-Rich Clays for Alkaline Activation Purpose: Mechanical, Thermal Activation in Red/Ox Atmosphere and Their Combination. *Appl. Clay Sci.* **2018**, *152*, 9–21. [CrossRef]

21. D'Elia, A.; Pinto, D.; Eramo, G.; Laviano, R.; Palomo, A.; Fernández-Jiménez, A. Effect of Alkali Concentration on the Activation of Carbonate-High Illite Clay. *Appl. Sci.* **2020**, *10*, 2203. [CrossRef]
22. D'Elia, A.; Clausi, M.; Fernández-Jiménez, A.; Palomo, A.; Eramo, G.; Laviano, R.; Pinto, D. Alkali-Activated Binary Binders with Carbonate-Rich Illitic Clay. *Polymers* **2023**, *15*, 362. [CrossRef]
23. Garcia Lodeiro, I.; Cristelo, N.; Palomo, A.; Fernández-Jiménez, A. Use of Industrial By-Products as Alkaline Cement Activators. *Constr. Build. Mater.* **2020**, *253*, 119000. [CrossRef]
24. Bernal, S.A.; Rodríguez, E.D.; Kirchheim, A.P.; Provis, J.L. Management and Valorisation of Wastes through Use in Producing Alkali-Activated Cement Materials. *J. Chem. Technol. Biotechnol.* **2016**, *91*, 2365–2388. [CrossRef]
25. Occhipinti, R.; Lanzafame, G.; Lluveras Tenorio, A.; Finocchiaro, C.; Gigli, L.; Tinè, M.R.; Mazzoleni, P.; Barone, G. Design of Alkali Activated Foamy Binders from Sicilian Volcanic Precursors. *Ceram. Int.* **2023**, *49*, 38835–38846. [CrossRef]
26. Hossain, M.U.; Ng, S.T.; Antwi-Afari, P.; Amor, B. Circular Economy and the Construction Industry: Existing Trends, Challenges and Prospective Framework for Sustainable Construction. *Renew. Sustain. Energy Rev.* **2020**, *130*, 109948. [CrossRef]
27. Espejel-Ayala, F.; Schouwenaars, R.; Durán-Moreno, A.; Ramírez-Zamora, R.M. Use of Drinking Water Sludge in the Production Process of Zeolites. *Res. Chem. Intermed.* **2014**, *40*, 2919–2928. [CrossRef]
28. Rozhkovskaya, A.; Rajapakse, J.; Millar, G.J. Synthesis of High-Quality Zeolite LTA from Alum Sludge Generated in Drinking Water Treatment Plants. *J. Environ. Chem. Eng.* **2021**, *9*, 104751. [CrossRef]
29. De Carvalho Gomes, S.; Zhou, J.L.; Li, W.; Long, G. Progress in Manufacture and Properties of Construction Materials Incorporating Water Treatment Sludge: A Review. *Resour. Conserv. Recycl.* **2019**, *145*, 148–159. [CrossRef]
30. Yang, J.; Ren, Y.; Chen, S.; Zhang, Z.; Pang, H.; Wang, X.; Lu, J. Thermally Activated Drinking Water Treatment Sludge as a Supplementary Cementitious Material: Properties, Pozzolanic Activity and Hydration Characteristics. *Constr. Build. Mater.* **2023**, *365*, 130027. [CrossRef]
31. Mañosa, J.; Cerezo-Piñas, M.; Maldonado-Alameda, A.; Formosa, J.; Giro-Paloma, J.; Rosell, J.R.; Chimenos, J.M. Water Treatment Sludge as Precursor in Non-Dehydroxylated Kaolin-Based Alkali-Activated Cements. *Appl. Clay Sci.* **2021**, *204*, 106032. [CrossRef]
32. Ferone, C.; Capasso, I.; Bonati, A.; Roviello, G.; Montagnaro, F.; Santoro, L.; Turco, R.; Cioffi, R. Sustainable Management of Water Potabilization Sludge by Means of Geopolymers Production. *J. Clean. Prod.* **2019**, *229*, 1–9. [CrossRef]
33. Geraldo, R.H.; Fernandes, L.F.R.; Camarini, G. Water Treatment Sludge and Rice Husk Ash to Sustainable Geopolymer Production. *J. Clean. Prod.* **2017**, *149*, 146–155. [CrossRef]
34. Messina, F.; Ferone, C.; Molino, A.; Roviello, G.; Colangelo, F.; Molino, B.; Cioffi, R. Synergistic Recycling of Calcined Clayey Sediments and Water Potabilization Sludge as Geopolymer Precursors: Upscaling from Binders to Precast Paving Cement-Free Bricks. *Constr. Build. Mater.* **2017**, *133*, 14–26. [CrossRef]
35. Nimwinya, E.; Arjharn, W.; Horpibulsuk, S.; Phoo-Ngernkham, T.; Poowancum, A. A Sustainable Calcined Water Treatment Sludge and Rice Husk Ash Geopolymer. *J. Clean. Prod.* **2016**, *119*, 128–134. [CrossRef]
36. Waijarean, N.; Asavapisit, S.; Sombatsompop, K. Strength and Microstructure of Water Treatment Residue-Based Geopolymers Containing Heavy Metals. *Constr. Build. Mater.* **2014**, *50*, 486–491. [CrossRef]
37. Suksiripattanapong, C.; Horpibulsuk, S.; Chanprasert, P.; Sukmak, P.; Arulrajah, A. Compressive Strength Development in Fly Ash Geopolymer Masonry Units Manufactured from Water Treatment Sludge. *Constr. Build. Mater.* **2015**, *82*, 20–30. [CrossRef]
38. Hwang, C.L.; Chiang, C.H.; Huynh, T.P.; Vo, D.H.; Jhang, B.J.; Ngo, S.H. Properties of Alkali-Activated Controlled Low-Strength Material Produced with Waste Water Treatment Sludge, Fly Ash, and Slag. *Constr. Build. Mater.* **2017**, *135*, 459–471. [CrossRef]
39. Babatunde, A.O.; Zhao, Y.Q. Constructive Approaches Toward Water Treatment Works Sludge Management: An International Review of Beneficial Reuses. *Crit. Rev. Environ. Sci. Technol.* **2007**, *37*, 129–164. [CrossRef]
40. Ahmad, T.; Ahmad, K.; Alam, M. Sustainable Management of Water Treatment Sludge through 3'R' Concept. *J. Clean. Prod.* **2016**, *124*, 1–13. [CrossRef]
41. Clausi, M.; Pinto, D. Valorisation of Water Potabilization Sludges as Precursors for Alkali-Activated Binders: Characterization and Feasibility Study. *Materials* **2023**, *16*, 1998. [CrossRef]
42. Ahmad, T.; Ahmad, K.; Alam, M. Sludge Quantification at Water Treatment Plant and Its Management Scenario. *Environ. Monit. Assess.* **2017**, *189*, 453. [CrossRef]
43. Lagaly, G.; Tufar, W.; Minihan, A.; Lovell, A. Silicates. In *Ullmann's Encyclopedia of Industrial Chemistry*; John Wiley & Sons, Ltd.: Hoboken, NJ, USA, 2000; ISBN 9783527306732.
44. Dell'Anna, L.; Laviano, R. Mineralogical and Chemical Classification of Pleistocene Clays from the Lucanian Basin (Southern Italy) for the Use in the Italian Tile Industry. *Appl. Clay Sci.* **1991**, *6*, 233–243. [CrossRef]
45. *ISO 13320*; Particle Size Analysis Laser Diffraction Methods. ISO: Geneva, Switzerland, 2020.
46. Rietveld, H.M. The Rietveld Method. *Phys. Scr.* **2014**, *89*, 98002. [CrossRef]
47. Bergmann, J.; Friedel, P.; Kleeberg, R. BGMN—A New Fundamental Parameters Based Rietveld Program for Laboratory X-Ray Sources, Its Use in Quantitative Analysis and Structure Investigations. *CPD Newsl.* **1998**, *20*, 5–8.
48. Doebelin, N.; Kleeberg, R. Profex: A Graphical User Interface for the Rietveld Refinement Program BGMN. *J. Appl. Crystallogr.* **2015**, *48*, 1573–1580. [CrossRef]
49. Lancellotti, I.; Catauro, M.; Ponzoni, C.; Bollino, F.; Leonelli, C. Inorganic Polymers from Alkali Activation of Metakaolin: Effect of Setting and Curing on Structure. *J. Solid. State Chem.* **2013**, *200*, 341–348. [CrossRef]

50. Duxson, P.; Provis, J.L.; Lukey, G.C.; Mallicoat, S.W.; Kriven, W.M.; Van Deventer, J.S.J. Understanding the Relationship between Geopolymer Composition, Microstructure and Mechanical Properties. *Colloids Surf. A Physicochem. Eng. Asp.* **2005**, *269*, 47–58. [CrossRef]
51. Santos, G.Z.B.; Melo Filho, J.A.; Pinheiro, M.; Manzato, L. Synthesis of Water Treatment Sludge Ash-Based Geopolymers in an Amazonian Context. *J. Environ. Manag.* **2019**, *249*, 109328. [CrossRef]
52. Ruiz-Santaquiteria, C.; Fernández-Jiménez, A.; Skibsted, J.; Palomo, A. Clay Reactivity: Production of Alkali Activated Cements. *Appl. Clay Sci.* **2013**, *73*, 11–16. [CrossRef]
53. Provis, J.L.; Duxson, P.; van Deventer, J.S.J. The Role of Particle Technology in Developing Sustainable Construction Materials. *Adv. Powder Technol.* **2010**, *21*, 2–7. [CrossRef]
54. Puertas, F.; Martínez-Ramírez, S.; Alonso, S.; Vázquez, T. Alkali-Activated Fly Ash/Slag Cements: Strength Behaviour and Hydration Products. *Cem. Concr. Res.* **2000**, *30*, 1625–1632. [CrossRef]
55. Baerlocher, C.H.; Barker, R.M. The Crystal Structure of Synthetic Zeolite F. *Z. Für Krist.* **1974**, *140*, 10–26. [CrossRef]
56. Arbel Haddad, M.; Ofer-Rozovsky, E.; Bar-Nes, G.; Borojovich, E.J.C.; Nikolski, A.; Mogiliansky, D.; Katz, A. Formation of Zeolites in Metakaolin-Based Geopolymers and Their Potential Application for Cs Immobilization. *J. Nucl. Mater.* **2017**, *493*, 168–179. [CrossRef]
57. Gualtieri, A.; Norby, P.; Artioli, G.; Hanson, J. Kinetics of Formation of Zeolite Na-A [LTA] from Natural Kaolinites. *Phys. Chem. Miner.* **1997**, *24*, 191–199. [CrossRef]
58. Rożek, P.; Król, M.; Mozgawa, W. Geopolymer-Zeolite Composites: A Review. *J. Clean. Prod.* **2019**, *230*, 557–579. [CrossRef]